Oxonol VI as an optical indicator for membrane potentials in lipid vesicles

H.-J. Apell and B. Bersch

Department of Biology, University of Konstanz, Konstanz (F.R.G.)

Experiments with large unilamellar dioleoylphosphatidylcholine vesicles were carried out in order to study the effect of membrane potential on the fluorescence of Oxonol VI. A partition equilibrium of dye between membrane and water was found to exist with a partition coefficient $\gamma \equiv c_{lipid}/c_{water}$ of about 19 000 (at zero voltage). In the presence of an inside-positive membrane potential, the negatively charged dye accumulates in the intravesicular aqueous space according to a Nernst equilibrium. This leads to an increased adsorption of dye to the inner lipid monolayer and to a concomitant increase of fluorescence. The fluorescence change can be calibrated as a function of transmembrane voltage by generating a potassium diffusion potential in the presence of valinomycin. The intrinsic fluorescence of the membrane-bound dye is not affected by voltage; the whole influence of voltage on the fluorescence results from voltage-dependent partitioning of the dye between water and membrane. The voltage dependence of the apparent partition coefficient can be quantitatively described by a three-capacitor model in which the dye is assumed to bind to adsorption planes located on the hydrocarbon side of the membrane/solution interface. Oxonol VI was found to be suitable for detecting changes of membrane potential associated with the activity of the $(Na^+ + K^+)$-ATPase in reconstituted vesicles. When ATP is added to the external medium, pump molecules with the ATP-binding side facing outward become activated; this results in a translocation of net positive charge towards the vesicle interior. Under this condition, fluorescence changes corresponding to (inside-positive) potentials of up to 150–200 mV are observed. After the build-up of the membrane potential, a quasi-stationary state is reached in which the pump current is compensated by a back-flow of charge through passive conductance pathways.

Introduction

Voltage-sensitive dyes are widely used for measuring membrane potentials of cells, cell organelles and membrane vesicles [1–4]. Experiments with intact cells usually require the detection of inside-negative potentials, and most voltage-sensitive dyes have been selected for this purpose. Oxonols (Fig. 1) belong to the few dyes which have been suc-

cessfully used in the measurement of inside-positive potentials [5–7]. Oxonols V, VI and VII have a pK near 4.2 and are anionic at physiological pH values [5,7]. They have been applied in studies with submitochondrial particles [8–11], chloroplasts [12,13], bacterial chromaffin granula [16], plasma-membrane vesicles [17,18] and (proteo) liposomes [7,19–22].

Oxonols are known to bind strongly to membrane vesicles; upon binding, both the absorption and the emission spectrum are shifted towards longer wavelengths [5,7]. Generation of an inside-positive membrane potential increases this red-

Correspondence: H.J. Apell, Department of Biology, University of Konstanz, D-7750 Konstanz, F.R.G.

oxonol V   R= -⟨○⟩
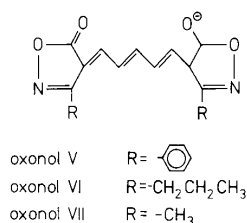oxonol VI   R=-$CH_2CH_2CH_3$
oxonol VII   R= -CH_3

Fig. 1. Structure of oxonols.

shift [14,15]. Furthermore, evidence has been obtained that oxonol anions easily permeate through lipid bilayers [6,7,14,23]. Based on these observations, it has been proposed that in the presence of an inside-positive potential, vesicles accumulate the anionic dye in the intravesicular aqueous space, which leads to enhanced binding of the dye to the membrane and to a concomitant spectral change [14,15,19].

In the follow, we describe a quantitative test of the proposed mechanism of voltage sensitivity of oxonol dyes, using large unilamellar dioleoylphosphatidylcholine vesicles prepared by detergent dialysis. We show that the experimental results indeed can be explained by the assumption of a voltage-dependent dye distribution between intra- and extravesicular aqueous space, provided that the theoretical model is suitably modified as to account for a direct field effect on the membrane–water partition coefficient of the dye.

The main incentive for this study was the possibility of using oxonol dyes as voltage indicators in studies with reconstituted $(Na^+ + K^+)$-ATPase vesicles [24]. Activation of Na^+,K^+-pump molecules inserted into the vesicle membrane by addition of ATP to the medium generates an inside-positive membrane potential. The analysis of the electrogenic effect of the pump requires a calibration of the observed spectral changes as a function of transmembrane voltage. Calibration experiments will be described below in which a Nernst potential for potassium was created in the presence of valinomycin. Furthermore, preliminary results from experiments with reconstituted $(Na^+ + K^+)$-ATPase vesicles will be presented.

Materials and Methods

Materials

Dioleoylphosphatidylcholine was obtained from Avanti Polar Lipids, Birmingham, AL, U.S.A.; Oxonol VI (bis(3-propyl-5-oxoisooxazol-4-yl)pentamethin oxonol) was from Molecular Probes, Junction City, OR, U.S.A., ATP (Sonderqualität) and valinomycin from Boehringer-Mannheim, Vanadate from Ventron, Karlsruhe. The phospholipid contents were determined by the Phospholipid B test from Wako Pure Chemical Industries, Ltd., Osaka, Japan. All other reagents were obtained from Merck (analytical grade). Dialysis tube was purchased from Serva, Heidelberg.

Vesicle preparations

Lipid vesicles were prepared from synthetic dioleoylphosphatidylcholine as described previously by a dialysis method producing homogeneous, unilamellar vesicles with an average outer diameter of 72 nm [24]. $(Na^+ + K^+)$-ATPase was prepared from outer medulla of rabbit kidneys using procedure C of Jørgensen [25], as described previously [24,26]. The specific activity was in the range of 1700–2100 μmol P_i per h per mg at 37°C. Reconstituted vesicles containing $(Na^+ + K^+)$-ATPase were prepared by cholate removement in 'buffer H' containing 30 mM imidazole, 1 mM L-cysteine, 1 mM EDTA, 5 mM $MgSO_4$ and various amounts of Na_2SO_4 and K_2SO_4. The average outer diameter of protein-containing vesicles has been previously determined to be about 96 nm [24].

Fluorescence measurements

Fluorescence experiments were carried out in a Perkin Elmer 650-40 fluorescence spektrophotometer. The thermostatically controlled cuvette holder was equipped with a magnetic stirrer. If not otherwise indicated, the excitation wavelength was set to 580 nm (slit width 20 nm) and the emission wavelength to 660 nm (slit width 5 nm). The Oxonol VI stock solution contained 3.16 mM dye in ethanol. From this stock solution dilutions were prepared by mixing with ethanol/water (1/5, v/v). Concentrations were chosen such that addition of 5 μl dye solution to the cuvette resulted in the desired final concentration (10–500 nM).

The dilute dye solutions were prepared daily. All fluorescence data were normalized with respect to a fluorescence standard.

The cuvette was filled with 1 ml buffer and equilibrated in the cuvette holder to the designed temperature. After the background fluorescence was measured, 5 μl of an Oxonol VI solution was added. After the fluorescence signal was constant, an aliquot of the vesicle suspension was added. Fluorescence changes, ΔF, caused by additions of reagents were determined as relative signal changes with respect to the fluorescence level, F_0, prior to the addition; they were corrected for the small dilution effect which was determined separately by adding a known amount of buffer solution. At the beginning and at the end of each experiment the temperature in the cuvette was controlled and the fluorescence signal of the standard was determined. If not otherwise indicated, the experiments were carried out at 20° C.

Results

Spectral properties as a function of dye and lipid concentration

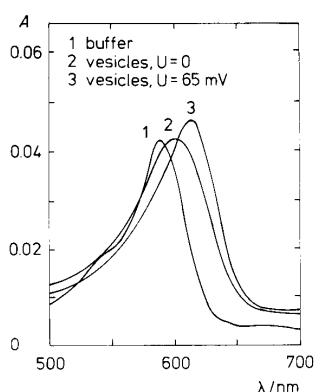The absorption and emission spectra of Oxonol

VI in free aqueous solution and in the presence of dioleoylphosphatidylcholine vesicles are represented in Figs. 2 and 3. It is seen that both the absorption and the emission peak are red-shifted when the dye interacts with the lipid and that a further red-shift occurs when an inside-positive membrane potential is generated. Furthermore, the fluorescence intensity increases (at an excitation wavelength of 580 nm) upon binding of the dye to the vesicles. As shown by Fig. 4, the peak wavelength λ_{max}, as well as the peak intensity F_{max} approach limiting values when the lipid concentration is increased at a constant (overall) concentration of Oxonol VI. This indicates that at the highest lipid concentrations used in the experiment (170 μg/ml) virtually all dye is bound to the vesicles.

Determination of the partition coefficient, γ, at zero voltage

The membrane–water partition coefficient, γ, of the dye is defined by

$$\gamma = \frac{n_1/V_1}{n_w/V_w} \tag{1}$$

Fig. 2. Optical absorbance (A) of a solution of 0.52 μM Oxonol VI in buffer H as a function of wavelength λ. Curve 1: dye in free buffer solution; curve 2; after addition of vesicles (50 μg lipid/ml); curve 3: as 2, in the presence of an inside-positive membrane potential of $U = 65$ mV. The membrane potential was created by a potassium gradient $[K^+]_i = 10$ mM, $[K^+]_0 = 140$ mM and 10 nM valinomycin to the medium; the value of U was calculated from Eqn. 6.
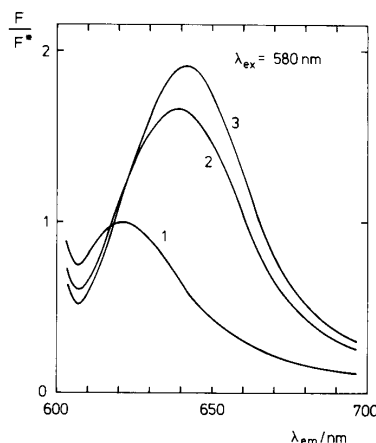
Fig. 3. Fluorescence intensity, F (normalized to the peak value, F^*, of curve 1), as a function of emission wavelength, λ_{em}. The excitation wavelength was 580 nm. Slid widths: 20 nm (excitation) and 5 nm (emission). Curve 1: 0.13 μM oxonol VI in buffer H; curve 2: after addition of vesicles (45 μg lipid/ml); curve 3: as 2, in the presence of an inside-positive membrane potential U of 36 mV created by adding K^+ and 10 nM valinomycin to the medium, the value of U was calculated from Eqn. 6.
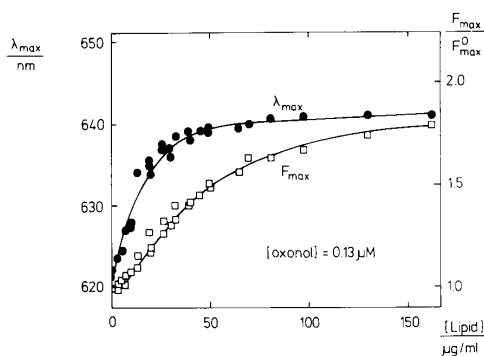
Fig. 4. Wavelength λ_{max} and fluorescence intensity F_{max} at the emission peak (excitation wavelength 580 nm) as a function of lipid concentration, at a constant (overall) dye concentration of 0.13 μM in buffer H. F_{max} is referred to the peak intensity F_{max}^0 at zero lipid concentration. The curves have been drawn to guide the eye.

Fig. 5. Fluorescence intensity F, divided by the total amount, n, of Oxonol VI in the fluorescence cuvette. F is referred to a fluorescence standard and is given in dimensionless units; n is expressed in nmol. The dependence of F/n on lipid concentration was measured at different concentrations of Oxonol VI: ●, 125 nM; ○, 250 nM; □, 500 nM. At all Oxonol concentrations the optical absorbance was so low that self-absorption, at a pathlength of 1 cm, was negligible. The curve represents a fit of Eqn. 3 using the following parameter values: $f_w = 0.55$ nmol^{-1}, $f_1 = 4.1$ nmol^{-1}, $\gamma = 19000$.

where n_1 and n_w are the amounts of dye (in mol) in the lipid phase and in the water phase and V_1 and V_w are the volumes of the lipid and water phases. If f_w and f_1 are the contributions of one mole of dye in the water and in the lipid to the observed fluorescence, the total fluorescence intensity, F, can be represented by

$$F = n_w f_w + n_1 f_1 \qquad (2)$$

In the following, F is referred to the fluorescence intensity measured with a fluorescence standard and is expressed in dimensionless units, so that f_w and f_1 have the dimension mol^{-1}. Eqns. 1 and 2 together give

$$F = n \frac{f_w V_w + \gamma f_1 V_1}{V_w + \gamma V_1} \qquad (3)$$

where $n = n_w + n_1$ is the total amount of dye in the fluorescence cuvette. Eqn. 3 predicts that the ratio F/n should be independent of oxonol concentration. This expectation is borne out by the experiments. As seen from Fig. 5, values of F/n for three different oxonol concentrations (125, 250 and 500 nM) fall nearly on the same line when F/n is plotted as a function of lipid concentration. At all oxonol concentrations, the optical absorbance of the solution is so low that self-ab-
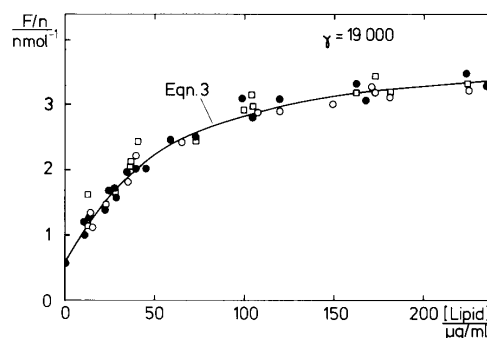
sorption, at a pathlength of 1 cm, is negligible. Eqn. 3 can be fitted to the experimentally observed dependence of F/n on lipid concentration, using the known values of V_w and V_1 (V_w is nearly to the total volume, $V = 1$ ml, of the vesicle suspension in the fluorescence cell, and V_1 is obtained from the concentration and the density, $\rho \approx 9$ mg/cm^3, of the lipid). The theoretical curve in Fig. 5 adequately describes the experimental results; from the fit the values of the fluorescence parameters, f_w and f_1, and of the partition coefficiency, γ, can be determined to be $f_w = 0.55$ nmol^{-1}, $f_1 = 4.1$ nmol^{-1} and $\gamma = 19000$.

Membrane potentials generated by K^+-concentration gradients

Membrane potentials may be generated by establishing a transmembrane K^+-concentration difference in the presence of valinomycin. At the beginning of the experiment, the K^+ concentration is the same in the intra- and extravesicular aqueous space, and the membrane is made selectively permeable by the addition of valinomycin. When the extravesicular K^+ concentration is increased, a Nernst potential for K^+,

$$U = \psi' - \psi'' = \frac{RT}{F} \ln \frac{c''}{c'} \qquad (4)$$

is created. ψ' and ψ'' are the intra- and extravesicular potentials, respectively, and c' and c'' are the corresponding K^+ concentrations; R is the gas constant, T the absolute temperature and F the Faraday constant. For the generation of the voltage U, an electric charge, Q, has to move across the membrane in order to charge up the membrane capacitance, AC_m (A is the total membrane area and $C_m \equiv 1 \ \mu F/cm^2$ is the specific membrane capacitance):

$$Q = AC_m U \tag{5}$$

The inward movement of K^+ associated with the establishment of the Nernst potential increases the intravesicular K^+ concentration from an initial value c_0' to a final value c'. If the membrane-permeable anionic dye is added to the medium, an additional transmembrane charge transport occurs, as the dye equilibrated between extra- and intravesicular aqueous space. This contribution of the dye to the membrane potential can, in general, not be neglected, although the effect may be small at low dye concentrations (see below). Under the condition that the volume of the intravesicular aqueous space is small compared to the total volume, the extravesicular K^+ concentration, c'', remains virtually constant during the build-up of the membrane potential. The intravesicular K^+ concentration changes, however, from the initial value, c_0', to a final value, c'. As shown in Appendix A, c' and c_0' are related by

$$c' = c_0' + C^* \ \ln \frac{c_0''}{c'} + \frac{(1+\sigma)c_D c_0''}{(1+a\sigma)c' + a(1+\sigma)c_0''} \tag{6}$$

$$C^* \equiv \frac{RT}{F^2} \cdot \frac{AC_m}{V'} \tag{7}$$

$$\sigma \equiv \gamma V_1/2V'; \quad a \equiv V'/V'' \tag{8}$$

C^* has the meaning of the concentration of univalent ions, referred to intravesicular volume, V', which are required to charge up the membrane capacitance to a voltage of $RT/F \approx 25$ mV. For a spherical vesicle of internal radius $r = 32$ nm, this concentration is given by $C^* = 3RTC_m/F^2 r \approx 250$ μM. The ratio, a, of intra- and extravesicular aqueous volume was always small; at the highest experimental lipid concentrations (about 200

μg/ml), a is of the order of 10^{-3}. For a spherical vesicle, the quantity σ may be estimated to be $\sigma = 3\gamma d/2r$, where d is the membrane thickness. With the experimentally determined partition coefficient, $\gamma \approx 19000$, σ becomes about 2000. Eqn. 6, which refers to an equilibrium state, is valid irrespective of the order of addition of valinomycin, K^+ and the dye. If c' is numerically evaluated from Eqn. 6, the membrane potential U can be calculated from Eqn. 4 (with $c'' = c_0''$).

Eqn. 6 limits the absolute magnitude of membrane potentials which can be generated by the K^+-gradient method. If the initial intravesicular potassium concentration is zero ($c_0' = 0$), the relation $C^* \ \ln(c_0''/c') = c'$ holds for small dye concentrations ($c_D \approx 0$). This yields, with $C^* = 250$ μM and $c_0'' = 140$ mM, a final intravesicular K^+ concentration of $c' \approx 0.5$ mM and, according to Eqn. 4, a membrane potential $U \approx 140$ mM. This value of U represents a practical upper limit of the voltage range in which fluorescence signals can be calibrated by the Nernst-potential method. In Fig. 6 the membrane potential, U, predicted from Eqns. 4 and 6 is plotted as a function of c_0''/c_0' for a fixed value $c_0'' = 140$ mM and a total dye concentration of either $c_D = 0$ or $c_D = 1$ μM. The
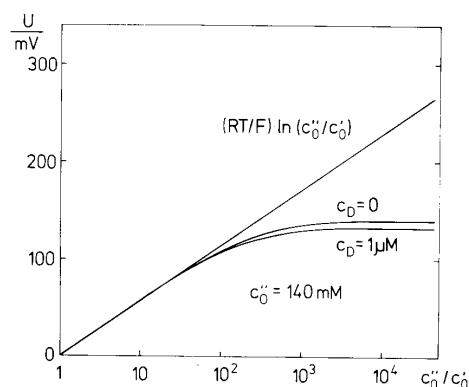

Fig. 6. Membrane potential, U, in the presence of a K^+ concentration difference. c_0' and c_0'' are the initial intra- and extravesicular K^+ concentrations, respectively, prior to the build-up of the membrane potential. The uppermost curve has been calculated from the Nernst equation assuming a constant intravesicular K^+ concentration. The lower curves have been obtained from Eqns. 4 and 6 with $c'' = c_0'' = 140$ mM, $a = 10^{-4}$, $\sigma = 1980$, and $C^* = 250$ μM.

difference of the curves for $c_D = 0$ and $c_D = 1$ μM represents the influence of the third term on the right side of Eqn. 6. It is seen that at concentrations as large as $c_D = 1$ μM the effect of dye translocation on membrane potential is small. In most experiments, however, c_D was much lower. This means that the term proportional to c_D in Eqn. 6 can be neglected under the conditions of our experiments.

Voltage-induced fluorescence changes

When an inside-positive membrane potential is generated by a K^+-concentration difference in the presence of valinomycin, the fluorescence intensity, F, increases (Fig. 7). The experimentally observed dependence of fluorescence intensity onlipid concentration was compared with the predict-

ions of the model, using again Eqn. 3. As shown by Fig. 7, the experimental results could be satisfactorily described by Eqn. 3 using voltage-independent values of the fluorescence parameters, f_w and f_l. The only quantity in Eqn. 3 which had to be varied with voltage in order to fit the experimental data was the partition coefficient, γ. This finding is consistent with the notion that the effect of voltage consists exclusively in changing the fraction of dye molecules which are bound to the membrane, whereas the average environment of a bound dye molecule remains virtually unchanged. With increasing inside-positive potentials, anionic dye molecules accumulate in the intravesicular solution. Since the external aqueous medium has a much larger volume, this leads to a net increase of the amount of bound dye. This increased dye-binding can be described by an apparent partition coefficient γ_{app} which is plotted in Fig. 8 as a function of voltage. A model which describes the voltage dependence of γ_{app} will be discussed later.
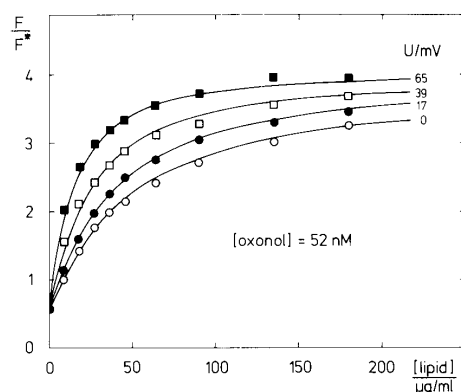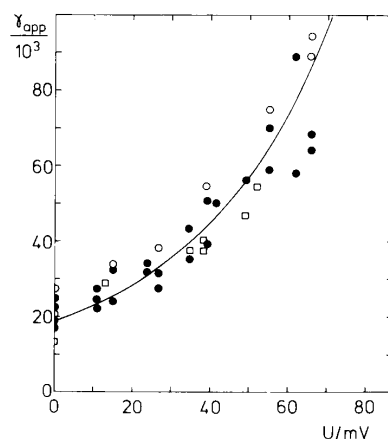
Fig. 7. Fluorescence intensity, F, as a function of lipid concentration for different membrane potentials, U. F^* is the intensity measured with a fluorescence standard instead of the cuvette. The membrane potential was generated by a K^+ concentration gradient in the presence of valinomycin. A suspension of vesicles formed in buffer H containing 10 mM K^+ were diluted with a solution of identical composition to yield the desired lipid concentration. To this solution was added 10 nM valinomycin. This usually resulted in a small signal change representing a constant offset of the fluorescence signal, F (see text). After the fluorescence signal became constant, the extravesicular K^+ concentration was increased by successive addition of small amounts of 3 M KCl. The value of U was calculated from Eqns. 4 and 6 with $a = 10^{-4}$, $\sigma = 1980$ and $c_d = 52$ nM. The curves have been calculated from Eqn. 3 using the following parameter values: $n/V_w = 52$ nM, $\rho_l = 9$ mg/ml, $f_w = 0.55$ nmol^{-1}, $f_l = 4.1$ nmol^{-1}, $\gamma = 19000$ (0 mV); 26400 (17 mV); 44600 (39 mV); 84000 (65 mV).

Fig. 8. Apparent partition coefficient, γ_{app}, as a function of membrane potential, U. γ_{app} was obtained by fitting Eqn. 3 to the experimental data represented in Fig. 7 and to additional data not shown in Fig. 7. The reconstitution of the $(Na^+ + K^+)$-ATPase vesicles was carried out with protein/lipid ratio (w/w) of 0.8/7.5. The theoretical curve was calculated from Eqn. 14 using the following parameter values: $\gamma = 19000$, $c_D = 130$ nM, $d = 4$ nm, $V'/V'' = 10^4$, $V_w \approx V''$. See legend of Fig. 7 for further explanations. $\bullet$, 13 nM Oxonol VI; $\bigcirc$, 130 nM Oxonol VI; $\square$, 13 nM Oxonol VI, vesicles containing $(Na^+ + K^+)$-ATPase.

If the voltage-induced fluorescence change, ΔF, results from a voltage-dependent redistribution of dye between water and membrane, the magnitude of ΔF should depend on lipid concentration. This is illustrated in Fig. 9, in which the relative fluorescence change, $\Delta F/F_0 \equiv [F(\mathrm{U}) - F(0)]/F(0)$, is plotted as a function of lipid concentration for a membrane calculated from Eqn. 3 with $\gamma_{\mathrm{app}}(U = 0) = 19\,000$ and $\gamma_{\mathrm{app}}(U = 65 \ \mathrm{mV}) = 84\,000$ taken from Fig. 8. The non-monotonic shape of the $\Delta F/F_0$ curve can be understood in the following way. At low lipid concentration the fluorescence signal is dominated by dye molecules dissolved in water, so that $\Delta F/F_0$ is small. At high lipid concentration most of the dye is already bound to te lipid meaning that the fluorescence change induced by an inside-positive voltage again is small. The theoretical curve in Fig. 9 agrees with the experimental results, although the scatter of the data points is too large to demonstrate unequiv-

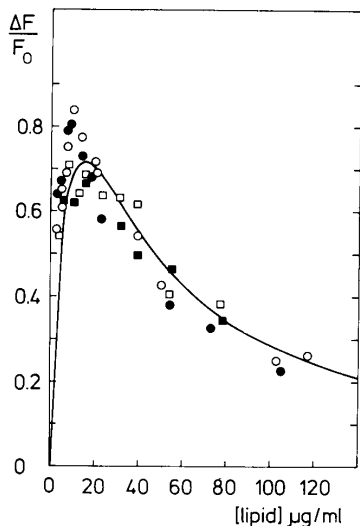ocally the decrease of $\Delta F/F_0$ at low lipid concentrations.

Calibration of fluorescence changes as a function of membrane potential

The relative fluorescence change $\Delta F/F_0 \equiv [F(U) - F(0)]/F(C)$ was measured in the voltage range between 0 and $+120$ mV (inside positive). These calibration experiments were carried out in the following way. To a suspension of vesicles with identical K^+ concentrations in the intra- and extravesicular medium was added 10 nM valinomycin. This resulted in a (usually negative) fluorescence change which was always smaller than 10%. A possible explanation of this signal offset which was only observed with protein-free vesicles consists in the assumption that a small membrane potential is present prior to the addition of valinomycin, which may result from the presence of residual cholate in the inner leaflet of the vesicle membrane [27]. Upon addition of valinomycin, the membrane potential drops to zero, corresponding to the symmetrical K^+ concentrations on either side of the vesicle membrane. The magnitude of the signal offset varied from vesicle preparation to vesicle preparation; however, when all fluorescence signals were referred to the fluorescence intensity after valinomycin addition, the calibration curves were reproducible.

In order to test whether the observed fluorescence changes are uniquely determined by membrane voltage, calibration experiments were carried out in which the same voltage was generated with different combinations of intra- and extravesicular potassium concentrations, keeping the ratio c'/c'' fixed and maintaining a constant total concentration, c_t, of Na^+ plus K^+ on both sides of the membrane. The result of these experiments is shown in Figs. 10A–C. As seen from Figs. 10A and 10B, the calibration curves measured with intravesicular K^+ concentrations of 1 and 10 mM are nearly the same, albeit with a small systematic deviation towards lower $\Delta F/F_0$ at $c_0' = 1$ mM. The total concentration of K^+ plus Na^+ in Figs. 10A and 10B was $c_t = 150$ mM; in Fig. 10C are shown experiments in which c_t was varied ($c_t = 75$, 150 and 300 mM). It is seen that the calibration curve is not significantly different at the different ionic strengths. Figs. 10A–C further show that the

Fig. 9. Fluorescence change, $\Delta F = F(U) - F(0)$, observed after generation of an inside-positive membrane potential of $U = 65$ mV, as a function of lipid concentration, $F_0 \equiv F(0)$ is the fluorescence intensity at zero voltage. The membrane potential, U, was created by an extravesicular K^+ concentration of 140 mM in the presence of 10 nM valinomycin; the intravesicular K^+ concentration was 10 mM. The value of U was calculated as described in the legend of Fig. 7. [Oxonol] (nM): ●, 62; ○, 125; □, 250; ■, 500.
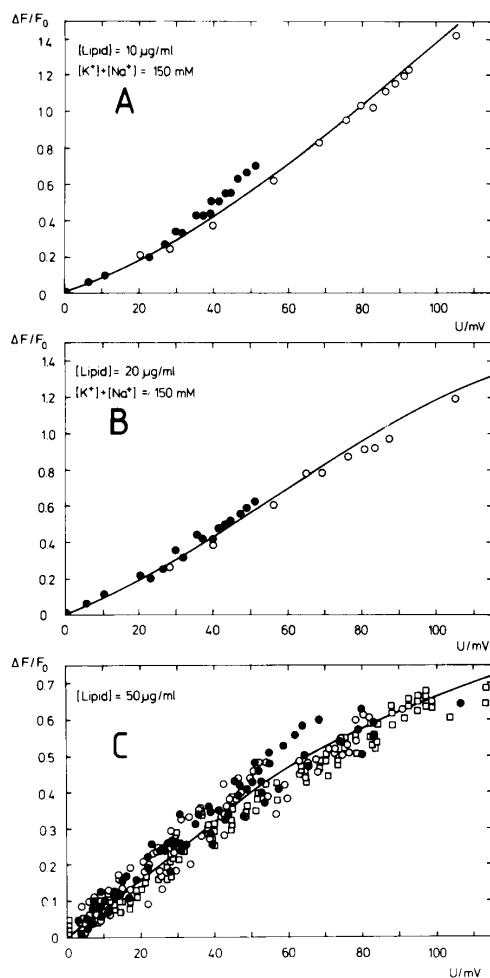
Fig. 10. Relative fluorescence change, $\Delta F/F_0 = [F(U) - F(0)]/F(0)$, as a function of transmembrane voltage, U. The voltage was generated by maintaining a K^+ concentration gradient across the vesicle membrane in the presence of 10 nM valinomycin. The value of U at a given initial intravesicular K^+ concentration, $c_0' = [K^+]_i^0$, was calculated from Eqns. 4 and 6, neglecting the term proportional to c_D in Eqn. 6. the concentrations of Oxonol VI ranged between 125 and 380 nM. $T = 20°$ C. The theoretical curves were calculated from Eqn. 9 with the following parameter values: (A) Lipid concentration 10 μg/ml; total concentration, c_t, of $Na^+ + K^+$ in the intra- and extravesicular medium, 150 mM; initial intravesicular K^+ concentration, 1 (O) or 10 mM (●). (B) As (A) but lipid concentration 20 μmol/ml. (C) Lipid concentration 50 μg/ml; c_t variable (75 (O), 150 (●) and 300 (□) mM); initial intravesicular K^+ concentrations between 1 and 10 mM.

calibration depends on lipid concentration, as may have been anticipated from Fig. 9. The continuous curves in Figs. 10A–C have been calculated on the basis of the theoretical model (Eqns. 9 and 14) to be discussed later.

At inside-negative potentials U the fluorescence signal $\Delta F/F_0$ tends to saturate already at small values of U, below ≈ -40 mV, as seen from Fig. 11. It is also seen from Fig. 11 that for $U < 0$ the fluorescence signal deviates from the theoretical curve (continuous line) which has been calculated using values of the model parameters determined from experiments at $U > 0$. The origin of this discrepancy is not clear so far.

In all experiments described so far, the dye was added to the extravesicular medium. A few experiments were carried out in which the dye was present already in the dialysis medium used for the formation of the vesicles. The same dye concentration (130 nM) was present in the fluorescence cuvette to which the vesicles were added. Under this symmetrical condition with respect to dye concentration, the calibration curve was found to be virtually the same as in the asymmetrical case. This observation is consistent with the assumption (on which the interpretation of our experiments is based) that Oxonol VI equilibrates across the vesicle membrane.
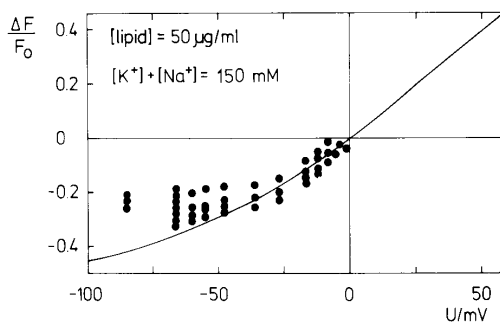

Fig. 11. Relative fluorescence change, $\Delta F/F_0$, at inside-negative membrane potentials, U. Vesicles loaded with 140 mM K^+ were suspended in a medium containing 10 nM valinomycin, 52 nM Oxonol VI and various K^+ concentrations, $c'' \leqslant 100$ mM. The total concentration of $Na^+ + K^+$ in the intra- and extravesicular medium was kept constant at 150 mM. The lipid concentration was 50 μg/ml. $T = 20°$ C.

Membrane potentials generated by the Na^+,K^+-pump

Reconstituted ($Na^+ + K^+$)-ATPase vesicles formed by detergent dialysis contain pump molecules of either orientation [28,29]. By adding ATP to the extravesicular medium, only those pumps with an outside-facing ATP-binding site become activated. Since the ($Na^+ + K^+$)-ATPase normally transports 3 Na^+ ions outward and 2 K^+ ions inward [30], activation of inside-out-oriented pumps should generate an inside-positive membrane potential in the vesicle [24]. An experiment demonstrating this electrogenic effect of the pump is shown in Fig. 12. After addition of 2.5 mM ATP to the vesicle suspension at a temperature of 11°C, the fluorescence starts to increase, reaching a plateau after about 80 s. From the plateau value of $\Delta F/F_0$ (≈ 0.8) and the calibration curve for 35 μg/ml lipid, the maximum voltage is estimated to be about 90 mV (inside positive). When vanadate, a potent inhibitor of the Na^+,K^+-pump [30] is added to the medium, the signal declines, approaching an asymptotic value with a time constant of about 200 s. (The fact that the fluorescence intensity drops below the starting value may result from a change of interfacial potential by
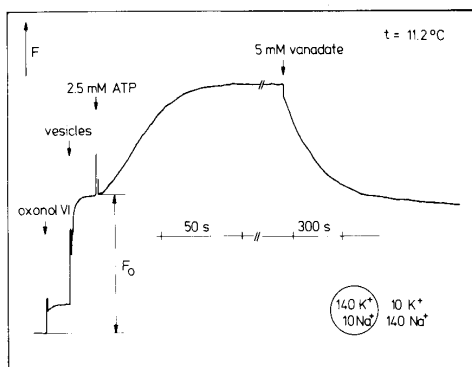

Fig. 12. Membrane potential generated by the Na^+,K^+-pump. Vesicles were reconstituted in buffer H containing 140 mM K^+ and 10 mM Na^+, as described before [24] and suspended in buffer H containing 140 mM Na^+ and 10 mMK$^+$. The average number of pump molecules with the ATP-binding site facing outward was determined to be $n \approx 1$. 52 nM Oxonol VI, 35 μg/ml lipid, 2.5 mM ATP and 5 mM vanadate were successively added. F is the fluorescence intensity. The temperature was 11.2°C.

vanadate binding, as reflected by the fast fluorescence change upon vanadate addition.) The decline of fluorescence intensity is likely to result from a decay of membrane voltage via the leakage conductance of the vesicle membrane. If this is true, then the time constant, τ, should be equal to C_m/G_m, where C_m and G_m are the specific capacitance and the specific conductance of the membrane, respectively. With $\tau \approx 200$ s and $C_m \approx 1$ μF/cm^2, G_m becomes about 5 nS/cm^2, which is reasonable value for a lipid bilayer [31]. From the initial slope of $\Delta F/F_0$ versus time t in Fig. 12, the initial rate of voltage change can be estimated to be $dU/dt \approx 1.75$ mV·s^{-1} which must be equal to $ne_0 v_0/AC_m$ where n is the average number of (outward oriented) pump molecules per vesicle, e_0 the elementary charge, v_0 the initial turnover rate and A the average area of the vesicle membrane. In the vesicle preparation used for the experiment of Fig. 12, n was determined from the potassium flux rate [24] to be about 1. This yields, with $A \approx 0.025$ μm^2 and $e_0 \approx 1.6 \cdot 10^{-19}$ C, an initial turnover rate of $v_0 = AC_m(dU/dt)/n_0 \approx 2.8$ s^{-1}. On the other hand, if v is the turnover rate in the quasi-stationary state in which the pump current is compensated by a backflow of charge through the membrane conductance G_m, the relation $ne_0 v = AG_m U_s$ holds where $U_s \approx 90$ mV is the stationary voltage. This gives $v = 0.058$ s^{-1}. Thus, the turnover rate, v, in the quasi-stationary state is about 50-times smaller than the initial turnover rate, v_0. The difference between v and v_0 is likely to reflect the voltage dependence of pumping rate [32].

When the experiment is carried out at a higher temperature (18°C), the initial rate of fluorescence change after ATP addition is much increased (Fig. 13). The fluorescence signal, F, maintains its plateau value only for a short time and then declines toward a much lower level. A likely explanation of the decline of F lies in the assumption that ATP-driven potassium extrusion results in a progressive reduction of intravesicular K^+ concentration which eventually leads to an inhibition of the pump followed by a decay of voltage via leakage pathways. From Figs. 13 and 10 the initial rate of voltage change may be estimated to be about 10 mV·s^{-1}, corresponding, for a spherical vesicle of internal radius $r = 40$ nm, to
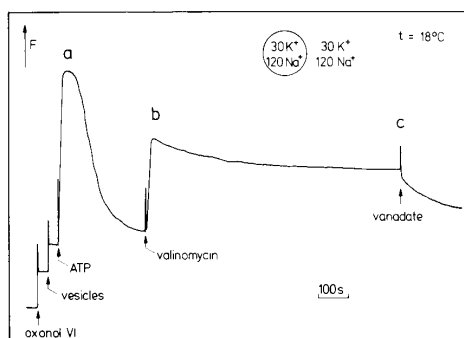
Fig. 13. Membrane potential generated by the Na^+,K^+-pump. Vesicles were reconstituted in buffer H containing 30 mM K^+ and 120 mM Na^+ and suspended in the same medium. 13 mM Oxonol VI, 8 $\mu g/ml$ lipid, 2.5 mM ATP, 10 nM valinomycin and 5 mM vanadate were added successively. $T = 18°$ C. a, b and c have been estimated to be about 160, 100 and 75 mV, respectively.

a K^+-depletion rate of $(3C_m/e_0 r) \cdot dU/dt \approx 0.2$ mM $\cdot$ s^{-1} (assuming that two K^+ ions are extruded per turnover). This means that the intravesicular K^+-concentration would drop within about 150 s from the initial value of 30 mM to nearly zero if the pumping rate v were to retain its initial value for this period of time. In reality, pumping is slowed down by the opposing effect of transmembrane voltage, which tends to increase the depletion time, t^*. The fact that the estimated value of t^* agrees approximately with the duration of the quasi-stationary period in Fig. 13 is consistent with the assumption that the decay of the fluorescence signal results from K^+ depletion of the vesicle. This assumption is further supported by the finding that, upon addition of valinomycin, the fluorescence increases again (Fig. 13), indicating the presence of an inward directed K^+-concentration gradient.

The relative fluorescence change, $\Delta F/F_0$, at the plateau of the fluorescence signal in Fig. 13 is about 2.7. Since this value exceeds the range of the calibration curve (Fig. 10), the voltage U corresponding to $\Delta F/F_0$ can only be estimated on the basis of the theoretical calibration curve calculated by fitting the model parameters to the experimental data at lower voltage. In this way the

voltage at the plateau of F in Fig. 13 is estimated to be approx. 160 mV.

The initial rate of fluorescence change after ATP addition has been measured at different temperatures. Using the calibration curve, the density of active pump molecules per vesicle and accounting for the membrane capacitance, the initial pumping rate, v_0, can be evaluated as a function of temperature. The results are plotted in Fig. 14 in the form of an Arrhenius diagram. From the slope of ln v_0 vs. $1/T$ the activation energy of the pump current is determined to be $E_a \approx 160$ kJ $\cdot$ mol^{-1}. Implicit in the determination of E_a is the assumption that the redistribution of the dye across the vesicle membrane is not rate limiting.

Under similar conditions the activation energy of the turnover rate was experimentally determined to be 115 kJ/mol using an indocyanine dye as potential indicator [24]. In order to test for a possible influence of Oxonol VI on the activation energy a number of control experiments was performed. In a first series of experiments the enzymatic activity of reconstituted $(Na^+ + K^+)$-
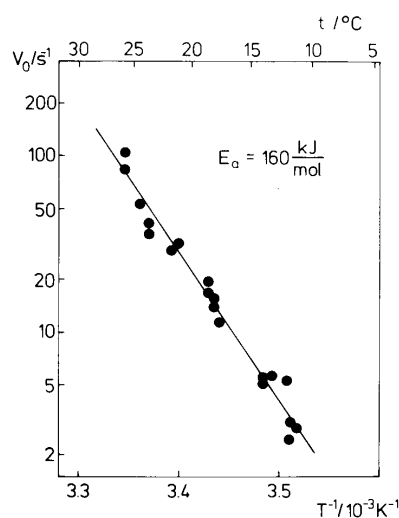

Fig. 14. Initial pumping rate, v_0 (referred to unit membrane area), as a function of reciprocal temperature. v_0 has been estimated from the initial rate of fluorescence change after ATP addition using the calibration curve (Fig. 10) and accounting for the membrane capacitance. E_a is the activation energy obtained from the Arrhenius relation.

ATPase was checked in the presence of different concentrations of Oxonol VI. At aqueous dye concentrations lower than 500 nM the enzymatic activity measured by the pyruvate kinase/lactate dehydrogenase assay [35] was not significantly influenced. In a second series of experiments, vesicles (with and without enzyme) containing 10 mM K^+ were diluted in an isoosmolar buffer with 140 mM K^+. Upon addition of valinomycin, the fluorescence signals increased to reach the level of the Nernst potential. The initial rate of fluorescence change was recorded at different temperatures. No significant temperature dependence was found in the range between $8°C$ and $25°C$. At $15°C$ and a valinomycin concentration of 20 nM the initial rate of voltage change was found to be about 30 mV/s. This rate is large compared to the rate of voltage rise observed after pump activation by ATP.

Marcus et al. [36] found strong effects of chain length and of the number of double bonds in the fatty-acid residue of the lipid onto the activation energy of reconstituted $(Na^+ + K^+)$-ATPase. These findings suggest a possible explanation of the increased activation energy. Oxonol VI, which is contained in the membrane in a ratio of 1/500 to 1/100 dyes per lipid molecules, could include a 'cholesterol-like' effect on membrane rigidity, or it may alter membrane thickness and interfere in this way with pumping activity.

Discussion

The results presented in this study show that the effect of transmembrane voltage on fluorescence of Oxonol VI in a vesicle suspension can be understood on the basis of a simple model. The experiments carried out at zero voltage indicated that a partition equilibrium exists between dye in water and dye adsorbed to the membrane. Upon adsorption, the fluorescence (at an excitation wavelength of 580 nm) increases by a factor of $4.1/0.55 \approx 7.4$. With a partition coefficient $\gamma \approx 19\,000$, a substantial fraction of the dye is bound to the membrane at lipid concentrations of the order of 10–100 $\mu g/ml$. In the presence of an inside-positive membrane potential, the negatively charged dye accumulates in the intravesicular aqueous space according to a Nernst equilibrium.

This leads to an increased adsorption of dye to the inner lipid monolayer and to a concomitant increase of fluorescence. This mechanism which has been previously discussed in the literature [14,15,19] is strongly supported by the quantitative analysis described in this paper.

Voltage dependence of the apparent partition coefficient

From the analysis of voltage-induced fluorescence changes as a function of lipid concentration (Fig. 7) it is found that the intrinsic fluorescence, f_1, of the membrane-bound dye is voltage-independent. The whole effect of voltage on the fluorescence F of the vesicle suspension can be described by a voltage-dependent apparent partition coefficient γ_{app} which enters into Eqn. 3:

$$F = n\frac{f_w V_w + \gamma_{app} f_1 V_1}{V_w + \gamma_{app} V_1} \qquad (9)$$

In the following, we show that the experimentally observed voltage-dependence of γ_{app} (Fig. 8) can be quantitatively described by the three-capacitor model depicted in Fig. 15, which has previously been used in the analysis of adsorption of lipophilic ions to lipid bilayers [34,35]. The dye is
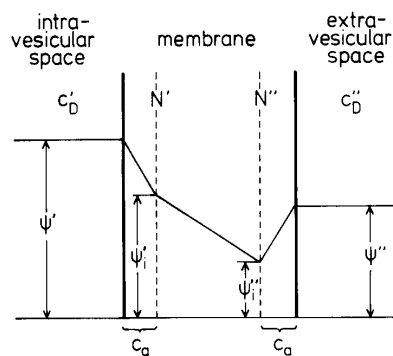

Fig. 15. Three-capacitor model used in analyzing the voltage dependence of the apparent partition coefficient γ_{app}. The dye is assumed to adsorption planes located symmetrically with respect to the centre of the membrane. C_a is the electrical capacitance between the adsorption plane and the adjacent aqueous solution. c'_D and c''_D are the aqueous dye concentrations. ψ', ψ'_i, ψ''_i and ψ'' the electric potentials, and N' and N'' the surface concentrations of bound dye.

assumed to bind to adsorption planes located on the hydrocarbon side of the membrane/solution interface. The surface concentrations, N' and N'', of bound dye (Fig. 15) which are referred to unit membrane area are given by

$$N' = \beta' \cdot c'_D, \qquad N'' = \beta'' \cdot c''_D \qquad (10)$$

where c'_D and c''_D are the aqueous dye concentrations. If ψ' and ψ'' are the electrical potentials in the intra- and extravesicular space and ψ'_i and ψ''_i the potentials in the adsorption planes (Fig. 15), the voltage dependence of the interfacial partition coefficients, β' and β'', may be expressed by

$$\beta' = \beta \exp(-u'); \qquad \beta'' = \beta \exp(-u'') \qquad (11)$$

$$u' \equiv F(\psi' - \psi'_i)/RT; \qquad u'' \equiv F(\psi'' - \psi''_i)/RT \qquad (12)$$

β is the value of β' and β'' at zero voltage. The dimensionless voltages, u' and u'', can be numerically evaluated on the basis of the three-capacitor model, as described in Appendix B. Since under equilibrium conditions $(U = 0, c'_D = c''_D = c_D)$ the relation $(N' + N'')/d = \gamma c_D$ holds, β and γ are connected by

$$\beta = \gamma d/2 \qquad (13)$$

with membrane thickness d (≈ 4 nm).

The fluorescence, F, of the vesicle suspension may be calculated introducing the relations $n_w = c'_D V' + c''_D V''$ and $n_1 = n - n_w = A(N' + N'')$ into Eqn. 2 (A is the total membrane area and V' and V'' are the volumes of the intra- and extravesicular space). Together with the Nernst relation $c'_D/c''_D = \exp(FU/RT) \equiv \exp(u)$, the fluorescence intensity, F, is obtained in the form of Eqn. 9, where γ_{app} is given by

$$\gamma_{app} \equiv \frac{(N' + N'')/d}{(c'_D V' + c''_D V'')/V_w} = \frac{\gamma V_w}{2} \cdot \frac{\exp(u - u') + \exp(-u'')}{V' \exp(u) + V''} \qquad (14)$$

In the limit $c_D \to 0$, u' and u'' in Eqns. 11 and 14 reduce to $u' \approx -u'' \approx (C_m/C_a)u$ (Appendix B). Since γ, V_w, V' and $V'' \approx V_w$ are known, Eqn. 14 can be fitted to the experimentally observed voltage dependence of γ_{app} (Fig. 8) using the numerically evaluated values of u' and u'' which depend

on the capacitance C_a (Fig. 15). It is seen from Fig. 8 that the theoretical curve which has been calculated with $\alpha \equiv C_a/C_m = 0.2$ adequately described the experimental data. The value of $\alpha = 0.2$ indicates that the adsorption plane is located away from the interface towards the hydrophobic interior of the membrane. This is consistent with the finding from ^{31}P-NMR experiments that Oxonol VI does not perturb the local motion of the phosphate group in phosphatidylcholine bilayers [20]. Eqns. 9 and 14 can also be used to fit the calibration curves, as shown by the theoretical curves in Figs. 10A–C.

Experiments with $(Na^+ + K^+)$-ATPase vesicles

Oxonol VI was found to be suitable for detecting changes of membrane potential associated with the activity of the Na^+,K^+-pump in reconstituted vesicles. When ATP is added to the external medium, pump molecules with the ATP-binding site facing outward become activated, which results in a translocation of net positive charge towards the vesicle interior. Under this condition large fluorescence changes are observed corresponding to inside-positive potentials of up to 150–200 mV. After the build-up of the membrane potential, a quasi-stationary state is reached in which the pump current is compensated by a back-flow of charge through passive conductance pathways. Experiments of this kind may be used for studying the current–voltage behaviour of the Na^+,K^+-pump.

Concluding remarks

From the foregoing analysis, a number of conclusions concerning the application of Oxonol VI for voltage measurements can be drawn. Since Oxonol VI distributes between intra- and extravesicular medium according to a Nernst equilibrium, inside-positive potentials can lead to a strong accumulation of the anionic dye and to high concentrations of bound dye in the inner lipid monolayer. This means that the simple mechanism discussed here for the dependence of optical properties on voltage can be operative only at sufficiently low dye concentrations. At high dye concentrations ($c_D > 1$ μM) additional phenomena, such as aggregation of dye molecules and self-

quenching of fluorescence, may be expected [15].

For an optimum voltage-response of the dye, the vesicle concentration is critical, as shown by Fig. 9. The optimum lipid concentration (which is independent of dye concentration) is found to be about 10–20 μg/ml. Calibration of the fluorescence signal as a function of voltage is meaningful only at a well-defined lipid concentration.

The response time of Oxonol VI after a fast voltage change is limited by the permeation rate of the dye across the membrane. In our experiments the response time was limited by the mixing time of reagents in the fluorescence cuvette and was less than 3 s. In experiments with bacterial chromatophores [14] Oxonol VI was found to respond in the time range of milliseconds to a light-induced change of membrane potential.

Appendix A

Derivation of Eqn. 6

We assume that initially the intra- and extravesicular K^+ concentrations are c_0' and c_0'', respectively, and that the membrane potential is zero. Upon addition of valinomycin and Oxonol VI, K^+ ions and dye anions move inward. After equilibration, the potassium concentrations in the intra- and extravesicular space are c' and c''. Since the total amount of K^+ in the system remains constant, the relation

$$c'V' + c''V'' = c_0'V' + c_0''V'' \tag{A-1}$$

holds, where V' and V'' are the volumes of the intra- and extravesicular aqueous spaces. Similarly, if $c_D V''$ is the total amount of dye which is initially added to the medium, the relation

$$c_D V'' = c_D' V' + c_D'' V'' + \frac{d}{2} A\gamma(c_D' + c_D'') \tag{A-2}$$

is fulfilled. c_D' and c_D'' are the dye concentrations in the intra- and extravesicular solutions after equilibration, A is the total membrane area, and d is the membrane thickness; the factor $(d/2)A\gamma(c_D' + c_D'')$ accounts for dye binding to either membrane/solution interface (γ is the partition coefficient defined by Eqn. 1). Implicit in Eqn. A-2 is the assumption that the partition equilibrium at

the interface is voltage-independent; this assumption is only approximately fulfilled, as discussed previously. We further assume that effects of electrical double-layers can be neglected in the presence of a sufficiently high concentration of inert electrolyte, and that the only permeable ion species (after addition of valinomycin) are K^+ and the dye anion. After equilibration, the membrane potential is given by

$$U \equiv \psi' - \psi'' = \frac{RT}{F} \ln \frac{c''}{c'} = \frac{RT}{F} \ln \frac{c_D'}{c_D''} \tag{A-3}$$

In order to build up this voltage, a charge $Q = AC_mU$ has to move across the membrane (A is the total membrane area, and C_m is the specific membrane capacitance). Q is given by the number of K^+ ions and dye anions which have entered the intravesicular aqueous space; an additional contribution to Q results from dye anions which became adsorebd to the inner membrane interface:

$$Q = F[(c' - c_0')V' + c_D'V' - c_D'A\gamma d/2] \tag{A-4}$$

This gives, together with $Q = AC_mU$:

$$c' = c_0' + C^* \ln \frac{c''}{c'} + c_D'(l + \sigma) \tag{A-5}$$

$$C^* \equiv RTAC_m/F^2V' \tag{A-6}$$

$$\sigma \equiv \gamma Ad/2V' = \gamma V_1/2V' \tag{A-7}$$

V_1 is the volume of the lipid phase. Eqns. A-1–A-5 together yield:

$$c'' = c_0'' - a(c' - c_0'); \qquad a \equiv V'/V'' \tag{A-8}$$

$$c' = c_0' + C^* \ln \frac{c''}{c'} + \frac{(l + \sigma)c_D c''}{(l + a\sigma)c' + a(l + \sigma)c''} \tag{A-9}$$

Eqn. A-8 and A-9 may be further simplified, since in the experiments described here, the volume of the intravesicular aqueous space is only a negligible fraction of the total volume. For a spherical vesicle of internal radius, r, and membrane thickness, d, the relation $a = y_1r/3\rho_1d$ holds, where y_1 and ρ_1 are the mass concentration and the density of the lipid, respectively. With $r \approx 50$ nm, $d \approx 5$ nm, $\rho_1 \approx 1$ g/cm^3 and $y_1 = 200$ μg/cm^3 (corresponding to the highest experimental lipid concentration), becomes of the order of 10^{-3}. This means that $c'' \approx c_0''$.

Appendix B

Boundary potentials generated by dye adsorption

When negatively-charged dye molecules bind to adsorption planes located on the hydrophobic side of the membrane/solution interface, boundary potentials are created. If ψ_i' and ψ_i'' are the electrical potentials in the adsorption planes and ψ' and ψ'' the potentials in the aqueous solutions (Fig. 15), the surface concentrations N' and N'' of dye molecules are given by

$$N' = \beta \exp(-u')c_D'; \quad u' \equiv \frac{\psi' - \psi_i'}{RT/F} \tag{B-1}$$

$$N'' = \beta \exp(-u'')c_D''; \quad u'' \equiv \frac{\psi'' - \psi_i''}{RT/F} \tag{B-2}$$

β is the interfacial partition coefficient and c_D' and c_D'' are the aqueous concentrations of the dye anion which are related by the Nernst equation:

$$\frac{c_D'}{c_D''} = \exp\left(\frac{\psi' - \psi''}{RT/F}\right) \equiv \exp(u) \tag{B-3}$$

On the basis of the three-capacitor model [33,34] depicted in Fig. 15, the voltages u', u'' and u are related to the charge densities q' and q'' in the adsorption planes:

$$q_i' = -FN' = \frac{RT}{F}(C_i u_i - C_a u') \tag{B-4}$$

$$q_i'' = -FN'' = \frac{RT}{F}(C_a u'' - C_i u_i) \tag{B-5}$$

$$u \equiv F(\psi' - \psi'')/RT \tag{B-6}$$

C_a is the capacitance between adsorption plane and aqueous phase and C_i is the capacitance between the adsorption planes. C_a and C_i are related to the total membrane capacitance, C_m, by

$$\frac{1}{C_m} = \frac{2}{C_a} + \frac{1}{C_i} \tag{B-7}$$

The total amount, n, of dye in the vesicle suspension is given by

$$n = c_D'V' + c_D''V'' + A(N' + N'') \tag{B-8}$$

V' and V'' are the volumes of the intra- and extravesicular aqueous solutions and A is the total

membrane area. Replacing β by the partition coefficient γ according to $\beta = \gamma d/2 = \gamma V_1/2A$ (V_1 is the total volume of the lipid) and using Eqns. B-1–B-8, one obtains

$$\frac{\gamma n d}{2N_0} \cdot \frac{(1-2\alpha)\exp(u-u')}{V'\exp(u)+V''+\gamma V_1[\exp(u-u')+\exp(-u'')]/2}$$

$$= -u + u'' + \frac{1-\alpha}{\alpha}u' \tag{B-9}$$

$$\frac{\gamma n d}{2N_0} \cdot \frac{(1-2\alpha)\exp(-u'')}{V'\exp(u)+V''+\gamma V_1[\exp(u-u')+\exp(-u'')]/2}$$

$$= u - u' + \frac{1-\alpha}{\alpha}u'' \tag{B-10}$$

$$\alpha \equiv C_a/C_m; \quad N_0 \equiv RTC_m/F^2 \tag{B-11}$$

Eqns. B-9 and B-10 can be used for numerical evaluation of the boundary potentials, u' and u'', which enter into the expression for the apparent partition coefficient γ_{app} (Eqn. 14). In the limit of low dye concentration ($n \to 0$), Eqns. B-9 and B-10 reduce to

$$u' \approx -u'' \approx \alpha u \tag{B-12}$$

as expected.

References

1 Bashford, C.L., Smith, J.C. (1978) Methods Enzymol. 55, 569–586
2 Waggoner, A.S. (1979) Annu. Rev. Biophys. Bioeng. 8, 47–68
3 Freedman, J.C. and Laris, P.C. (1981) Int. Rev. Cytol. Suppl. 12, 177–246
4 Waggoner, A.S. (1985) in The Enzymes of Biological Membranes, 2nd Edn. (Martonosi, A.N., ed.), Vol. 3, pp. 313–331, Plenum Press, New York
5 Smith, J.C., Russ, P., Cooperman, B.S. and Chance, B. (1976) Biochemistry 15, 5094–5105
6 Waggoner, A.S., Wang, C.H. and Tolles, R.L. (1977) J. Membrane Biol. 33, 109–140

494

7 Bashford, C.L., Chance, B., Smith, J.C. and Yoshida, T. (1979) Biophys. J. 25, 63–85
8 Bashford, C.L. and Thayer, W.S. (1977) J. Biol. Chem. 252, 8459–8463
9 Pringle, M.J. and Sanadi, D.R. (1984) Membrane Biochem. 5, 225–241
10 Smith, J.C. and Chance, B. (1979) J. Membrane Biol. 46, 255–282
11 Smith, J.C., Hallidy, L. and Topp, M.R. (1981) J. Membrane Biol. 60, 173–185
12 Schuurmans, J.J., Casey, R.P. and Kraayenhof, R. (1978) FEBS Lett. 94, 405–409
13 Admon, A., Shahak, Y. and Avron, M. (1982) Biochim. Biophys. Acta 681, 405–411
14 Bashford, C.L., Chance, B. and Prince, R.C. (1979) Biochim. Biophys. Acta 545, 46–57
15 Beeler, T.J., Farmen, R.H. and Martonosi, A.N. (1981) J. Membrane Biol. 62, 113–137
16 Scherman, D. and Henry, J.P. (1980) Biochim. Biophys. Acta 599, 150–166
17 Perlin, D.S., Kasamo, K., Brookers, R.J. and Slayman, C.W. (1984) J. Biol. Chem. 259, 7884–7892
18 Rasi-Caldogno, F., Pugliarello, M.Ch. and De Michelis, M.I. (1985) Plant Physiol. 77, 200–205
19 Krab, K., Van Walraven, J.S., Scholts, M.J.C. and Kraayenhof, R. (1985) Biochim. Biophys. Acta 809, 228–235
20 Bammel, B.P., Brand, J.A., Simmons, R.B., Evans, D.E. and Smith, J.C. (1987) Biochim. Biophys. Acta 896, 136–152
21 Navarro, J. and Essig, A. (1984) Biophys. J. 46, 709–717
22 Van Walraven, H.S., Krab, K., Hagendoorn, M.J.M. and Kraayenhof, R. (1985) FEBS Lett. 184, 96–99
23 Waggoner, A.S. (1976) J. Membrane Biol. 27, 317–334
24 Apell, H.-J., Marcus, M.M., Anner, B.M., Oetliker, H. and Läuger, P. (1985) J. Membrane Biol. 85, 49–63
25 Jørgensen, P.L. (1974) Methods Enzymol. 32, 277–290
26 Anner, B.M., Marcus, M.M. and Moosmayer, M. (1984) in Enzymes, Receptors and Carriers of Biomembranes (Azzi, A., Brodbeck, U. and Zahler, P., eds.), p. 81–99, Springer Verlag, Heidelberg
27 Ueno, M., Tanford, C. and Reynolds, J.A. (1984) Biochemistry 23, 3070–3076
28 Anner, B.M. (1985) Biochim. Biophys. Acta 832, 319–334
29 Anner, B.M. (1985) Biochim. Biophys. Acta 832, 335–353
30 Glynn, I.M. (1985) in The Enzymes of Biological Membranes, 2nd Edn. (Martonosi, A.N., ed.), Vol. 3, pp. 35–114, Plenum Press, New York
31 Hanai, T., Haydon, D.A. and Taylor, J. (1964) Proc. R. Soc. London, Ser. A 281, 377–391
32 Läuger, P. and Apell, H.-J. (1986) Eur. Biophys. J. 13, 309–321
33 Markin, V.S., Grigorev, P.A. and Yermishkin, L.N. (1971) Biofizika 16, 1011–1018
34 Andersen, O.S., Feldberg, S., Nakadomari, H., Levy, S. and McLaughlin, S. (1978) Biophys. J. 21, 35–70
35 Schwartz, A., Nagano, K., Nakao, M. Lindenmayer, G.E. and Allen, J.C. (1971) Methods Pharmacol. 1, 361–388
36 Marcus, M.M., Apell, H.-J., Roudna, M., Schwendener, R.A., Weder, H.-G. and Läuger, P. (1986) Biochim. Biophys. Acta 854, 270–278